PCCP

Accepted Manuscript

ROYAL SOCIETY OF CHEMISTRY

www.rsc.org/pccp

Journal Name

RSCPublishing

COMMUNICATION

A DFT+U study of NO evolution at reduced CeO_2(110)

Cite this: DOI: 10.1039/x0xx00000x

Jie Zhang,[ab] Xue-Qing Gong[ab*] and Guanzhong Lu[a*]

Received 00th January 2012,
Accepted 00th January 2012

DOI: 10.1039/x0xx00000x

www.rsc.org/

NO adsorption, diffusion and reaction at reduced CeO_2(110) were studied by density functional theory calculations. NO accommodated by O vacancy can readily diffuse via alternative NO_2 formation and dissociation, facilitating N_2O_2 formation and subsequent reduction to N_2. Rare earth ceria plays an important catalytic role in both static and dynamic ways by tuning the electron distribution in adsorbates and reacting molecules.

Gaseous nitrogen oxides (NO_x) from automobile exhaust emission and industrial combustion caused serious environmental problems including particulate pollution, acid rain, urban photochemical smog and ozone layer depletion, which brought big threat to human health and ecosystem over the past century. For this reason, NO_x emission control becomes extremely urgent and has drawn extensive attention. It is largely determined by efficient vehicle engines as well as improved NO_x degradation ($deNO_x$) techniques. The selective catalytic reduction (SCR)[1] and NO_x storage reduction (NSR)[2] are two widely used commercial approaches for $deNO_x$. However, from economic and environmental points of view, direct NO_x degradation is of prior importance since no reductant is needed, and accordingly, side reactions for unwanted products can be highly inhibited.[3, 4]

Rare earth cerium dioxide (ceria, CeO_2) based materials have been used as the important component of three-way catalysts (TWC) for vehicle emission control for several decades.[5-8] Its unique performance in dealing with hazard exhaust can be attributed to the fact that (i) CeO_2 exhibits high oxygen storage capacity (OSC) as oxygen buffer for storing or releasing oxygen when needed, which is mainly due to its small surface oxygen vacancy (O_v) formation energies;[9, 10] (ii) cerium has the characteristic highly localized 4*f* orbital, which may tune the distribution of catalytic sites, *e.g.* oxygen vacancies, especially in the case of surface redox reactions.[11-13] Daturi *et al.*[14] studied the reduction mechanism of NO adsorption and decomposition at pre-reduced ceria. They found that the $deNO_x$ activity in this system is closely related to the amount of oxygen vacancies at surfaces. Accordingly, they proposed the direct NO dissociation mechanism that two oxygen of two NO molecules refilled two adjacent oxygen vacancies and the two nitrogen then combined to give N_2. In another early study, Conesa and co-workers[15] also studied NO reaction at CeO_2 containing surface oxygen vacancies by electron paramagnetic resonance (EPR) and Fourier transform infrared spectroscopy (FTIR) measurement. From FTIR spectra, formation of intermediate species such as hyponitrites, nitrites and nitrates upon NO adsorption was detected. Moreover, for the decomposition process of NO at pre-treated CeO_2, N_2O was also found to occur, indicating that active surface sites containing associated oxygen vacancies might be responsible for NO reduction.[14] In addition, wide range of studies further showed that the activity of CeO_2 for direct NO degradation can be largely improved through Mn[16, 17], La and Y[18] doping, which may help increase the population of oxygen vacancies.

It is then widely believed that the presence of sufficient surface O_v, especially associated ones, are key to initiating NO (co-)adsorption and subsequent reactions for N_2 formation. Among the three low index facets of ceria, CeO_2(110) has been found to give the lowest O_v formation energy through density functional theory (DFT) calculations and is, therefore, considered to be more likely to give rise to O_v.[10] Accordingly, CeO_2(110) surface was expected to be highly active in catalytic reaction by providing more reacting surface oxygen and oxygen vacancies. For example, the experimental studies conducted by Li and co-workers[19] showed that, by exposing more {110} facets, the well-defined ceria nano-rods can exhibit improved catalytic activity toward CO oxidation. Our previous calculation work also showed that O_2 prefers to adsorb at reduced CeO_2(110), since it gives open topological structure that helps accommodate adsorbates at Ce cations.[20] In another recent work, we further calculated the direct reaction between surface O and gas-phase CO at different CeO_2 surfaces and found that since the three-fold coordinated O (O_{3c}) at CeO_2(110) binds with two unsaturated Ce while that at CeO_2(111) binds with three, it gives higher reactivity.[12]

Though a mass of experiment implied that ceria based materials have good catalytic performance for NO_x elimination and CeO_2(110) has been shown to give remarkable activity, the investigation into the detailed processes and unique role of this surface in NO activation and reaction is still limited. In this communication, these issues are tackled through systematic density functional theory calculations corrected by on-site Coulomb interaction (DFT+U) (see Supporting Information for details). In particular, by determining the

energetic and dynamic properties of O_v together with interacting NO, we are able to elucidate the catalytic process in NO_x degradation.

Crystalline ceria (110) surface has interesting structural feature that, from the side view, the whole surface slab can be taken as the cross packed arrays of flat O-Ce-O rows (see Figs. 1(a) and (b)). It exposes six-fold coordinated Ce (Ce_{6c}) and three-fold coordinated O (O_{3c}) on the top. In order to study the evolution of NO_x species at CeO_2(110), we first calculated NO adsorption on both the stoichiometric and reduced surfaces. From the calculation results summarized in Table 1 and Fig. S1, we can see that among the various adsorption sites tested at stoichiometric CeO_2(110) (see Fig. S1(a)-(d)), the one on-top of O_{3c} is the most favourable, though it gives NO adsorption energy (E_{ad}) of ~0.4 eV only, which is similar to what Yang *et al.*[21] reported in an early study. By contrast, on the defected surface with a single O_v, NO adsorption energy was determined to be increased to 0.83 eV. From the calculated adsorption structure (see Fig. S1(e)), we can clearly see that the NO now takes a horizontal configuration at the vacancy site. According to many experimental results, NO_2 usually occurs at the surface during NO temperature programmed desorption measurement.[22] In fact, from our calculations we also found that adsorbed NO can readily react with an O_{3c} at the adjacent CeO_2 row to form NO_2 and this process is exothermic by 0.57 eV (see Table 1 and Fig. S1(f)).

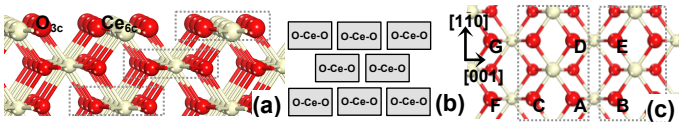

Fig. 1 Structure of CeO_2(110) surface (a: side view; b: cross packed diagram; c: top view). Ce is in white and O in red. Different O_{3c} are labeled in (c).

Table 1. Calculated NO adsorption energies at clean and defected CeO_2(110)

			NO				2NO	
		Clean surface			Single O_v		Double O_v	
Site	O_{3c}	Ce_{6c}	A-C	A-B	NO	NOO_{3c}	A-B	A-D
E_{ad} / eV	0.41	0.18	0.19	0.05	0.83	1.40	5.03	3.93
Figure	S1(a)	S1(b)	S1(c)	S1(d)	S1(e)	S1(f)	S1(g)	S1(h)

For the co-adsorption and reaction of two NO molecules, two different pairs of O vacancies, one along the [001] and the other along the [1$\bar{1}$0] direction, were first considered in this work. In both cases, the co-adsorbed NO at the pair of vacancy can easily combine to form N_2O_2 dimer. The calculated adsorption energy (with respect to two separate NO in gas phase) is as high as 5.03 eV for the dimer across two CeO_2 rows ([001], see Fig. S1(g)) and it is 3.93 eV for the dimer at one CeO_2 row ([1$\bar{1}$0], see Fig. S1(h)). It is then obvious that N_2O_2 could be precursor for deNO_x, and after consecutive N-O bond cleavage, N_2 might be able to form at the surface.

In order to verify the actual distribution pattern of O vacancies, we then performed systematic calculations of single and pair of O vacancies, and the results are summarized in Table S1. By removing different pairs of neighbouring surface O, *i.e.* O_A-O_B, O_A-O_C, O_A-O_D and O_A-O_E (see Fig. 1(c)), we were able to obtain all the possible pairs of associated O vacancies. From calculations, we found that the isolated single O vacancy, as well as the vacancy in these pairs (except O_A-O_C), can undergo heavy relaxation to give rise to the so-called split vacancy, which is about 0.15 eV more stable than the slightly relaxed single vacancy.[23, 24] Nevertheless, from Table S1, we can clearly see that except the O_A-O_E vacancy forming energy is 3.52 eV, *i.e.* giving a cost of 1.76 eV per vacancy, all the vacancy pairs are less stable than the isolated ones (1.87 eV, see Table S1). In particular, the O_A-O_B and O_A-O_D pairs, which were previously considered for co-adsorption of two NO are quite unfavourable. These results clearly indicate that from the thermodynamic point of view, the surface O vacancies tend to avoid from each other, and the vacancy dimers (O_A-O_B and O_A-O_D) may not occur natively at the CeO_2(110) surface.

Besides its thermodynamic stabilities, we also studied the dynamics of O vacancy by calculating its diffusion at the CeO_2(110) surface, which in fact was also proposed to affect the redox processes at CeO_2.[14, 25] By removing O_A, we can obtain a single O vacancy, for which the in-coming movement of one of the three nearest neighbouring O, namely O_B, O_C and O_D, actually corresponds to the diffusion of the vacancy along different directions. In particular, the movement of O_B and O_C to the vacancy can be taken as the diffusion of the vacancy along [001] and that of O_D as the vacancy diffusion along [1$\bar{1}$0].

For O_B movement to vacancy of O_A, we performed a series of constrained calculations by fixing its x coordinates at different values in between those for the O at site B and after filling the vacancy at site A. The transition state was determined for the diffusing O at the middle of the pathway and the barrier was estimated to be 0.41 eV (see Fig. S2, blue line). For the vacancy diffusion from site A to C, we determined the whole pathway with similar constrained calculations (see Fig. S2, red line). However, it needs to be mentioned that the split vacancy appears to be the intermediate state of the pathway, and the barriers for its formation from and transformation to the single vacancy were calculated to be 0.17 and 0.30 eV only, respectively.

For the O vacancy diffusion along [1$\bar{1}$0] direction, we were able to obtain the corresponding energy profile again by fixing the y coordinate of O_D and calculating a series of images along the pathway for O_D to move to the vacancy at site A (see Fig. S2, green line). We can see that O_D needs to overcome an extremely high barrier of ~1.8 eV to fill the vacancy directly. We also considered the indirect vacancy diffusion via a subsurface vacancy (see Fig. S2, purple line), and the barrier was determined to be as high as 1.48 eV, simply due to the fact that the subsurface O vacancy at CeO_2(110) gives the formation energy of ~2.6 eV, nearly 1 eV higher than that of the top-surface one. Therefore, it is also difficult for O vacancy to diffuse through such two-step pathway, which is very different from the case at CeO_2(111).[26]

The above results then suggest that the O vacancy diffusion along [001] direction is relatively easy, while that along [1$\bar{1}$0] is rather difficult to occur under mild conditions. In addition, considering that the O vacancy diffusion barrier in the bulk is also quite small (~0.5 eV),[27] one may expect that diffusion into the bulk can compete with that along [1$\bar{1}$0] as well. In other words, the diffusion of O vacancies would be partially inhibited at CeO_2(110), which further reduces the chance for the formation of associated vacancies.

However, considering that single NO can adsorb at an isolated O vacancy and react with neighbouring lattice oxygen to form NO_2, we then tested the possibility of NO diffusion, after its adsorption at O vacancy, through alternative NO_2 formation and dissociation. First, we calculated the reaction of NO adsorbed at the O vacancy at site F (AD1, see Fig. 2(a); Fig. S1(e)) with the nearest O in the neighbouring CeO_2 row (O_C). NO only needs to overcome the barrier of 0.16 eV (TS1) to give rise to the NO_2 bridging two CeO_2 rows (IM1; Fig. S1(f)). Then, this NO_2 can break the original N-O bond of NO with a barrier of 0.72 eV (TS2), and as the result, the newly formed NO appears to adsorb at a vacancy of sites C (AD2). Such NO can continue to react with O_A at the same CeO_2 row, and the corresponding reaction barrier to form such NO_2 (IM2) sitting on top of the row is 0.36 eV only (TS3). This NO_2 can again break the

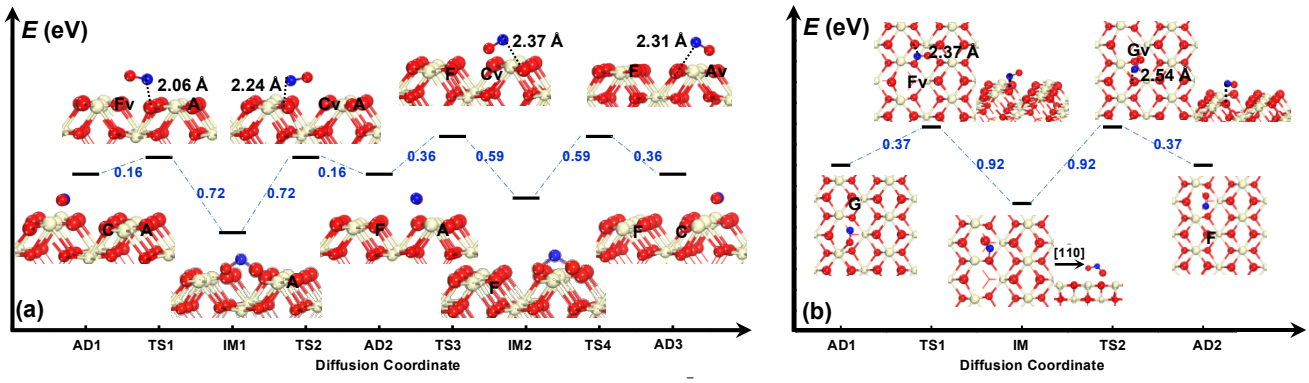

Fig. 2 Calculated energy profiles and key states of NO diffusion along [001] (a) and [1$\bar{1}$0] (b) directions on defected CeO_2(110). NO adsorption at O_F vacancy is set to energy zero.

former N-O bond to be reduced to NO, and the corresponding barrier was calculated to be 0.59 eV (TS4). Finally, this NO occurs just like the one adsorbed at the O vacancy at site A (AD3). From the calculated energetics presented in Fig. 2(a), we can conclude that the NO adsorption and diffusion along [001] direction at the reduced CeO_2(110) can readily occur.

Besides NO migration along [001], we also calculated similar process along [1$\bar{1}$0]. For the initial state, we still considered the adsorption of NO at the O vacancy of site F with the adsorption energy of 0.83 eV (AD1, see Fig. 2(b)). It then needs to overcome the barrier of 0.37 eV (TS1) only to combine with the neighbouring lattice O (O_G) to form a NO_2 (IM), and this adsorption state is 0.55 eV more stable than that of NO. Afterwards, the adsorbed NO_2 breaks the original N-O bond, leaving the O to fill the vacancy at site F(AD2), and the newly formed NO now appears move along the [1$\bar{1}$0] direction to sit at the vacancy of site G.

From the above calculation results, we can clearly see that, different from the diffusion of O vacancy alone, its migration together with adsorbed NO would be preferable to occur along both directions at the reduced CeO_2(110). It then suggests that though the O vacancies may not occur side-by-side natively at the surface, NO molecules adsorbed at isolated vacancies may still be able to move freely and involve in combination reactions when they get close to each other. For the two NO sitting side-by-side at the O vacancies along the [1$\bar{1}$0] direction (IS, see Fig. 3(a)), the barrier for them to combine at the N end is only 0.16 eV (TS1) and the as-produced N_2O_2 dimer can strongly bind at the centre of the vacancy pair in a chelating configuration (IM1). The barrier for this N_2O_2 to break one N-O bond, leaving the O to fill one vacancy, is only 0.61 eV (TS2), and the resulting N_2O only weakly adsorbs at the remaining O vacancy (IM2). The N_2O needs to overcome another small barrier of 0.49 eV to leave its O to the vacancy, and as the result, N_2 can form in the gas-phase above a fully oxidized CeO_2(110) (FS).

For the reaction between two NO at neighbouring CeO_2 rows, we considered the initial state, in which the two NO, rather than side by side, are at the second nearest positions (IS, see Fig. 3(b)), simply because that such A-E site vacancy pair configuration is rather favourable (see Table S1). As we have illustrated in Fig. 3(b), one NO molecule at the vacancy first reacts with the O at the neighbouring row to form a bridging NO_2 (IM1) with the barrier of 0.26 eV only (TS1), which was also expected to be an important step in NO reduction according to some experimental measurements.[28, 29] This NO_2 can readily react with the NO at the other vacancy to form an N_2O_3 intermediate species (IM2) with barrier of 0.29 eV (TS2), which is also consistent with the experimental finding that N_2O_3 species can be observed over Ce-exchanged mordenite catalyst after NO adsorption.[30] This N_2O_3 further dissociates to the same N_2O_2 species (IM3 in Fig. 3(b)) as in the former case of reaction along the same CeO_2 row (IM1 in Fig. 3(a)). The dissociation barrier was calculated to be 1.13 eV, which appears to be the highest one in these processes. The rest of the reaction following N_2O_2 formation would then be the same as those shown in Fig. 3(a).

In the above, the evolution of NO molecules at reduced CeO_2(110) has been comprehensively calculated by taking into consideration of their adsorption, migration, combination and dissociation. From the calculated energetics of the corresponding elementary steps (Figs. 2-3), we are able to tell that NO can preferably adsorb at surface O vacancy and by alternatively forming NO_2 with nearby lattice O and dissociating into NO and O to fill the original O vacancy, the adsorbed NO can diffuse along any directions at the surface. Moreover, two NO adsorbed at isolated vacancies, when getting close to each other from different directions, can also combine to form N_2O_2 dimer, which then dissociates to give rise to the desired product of N_2.

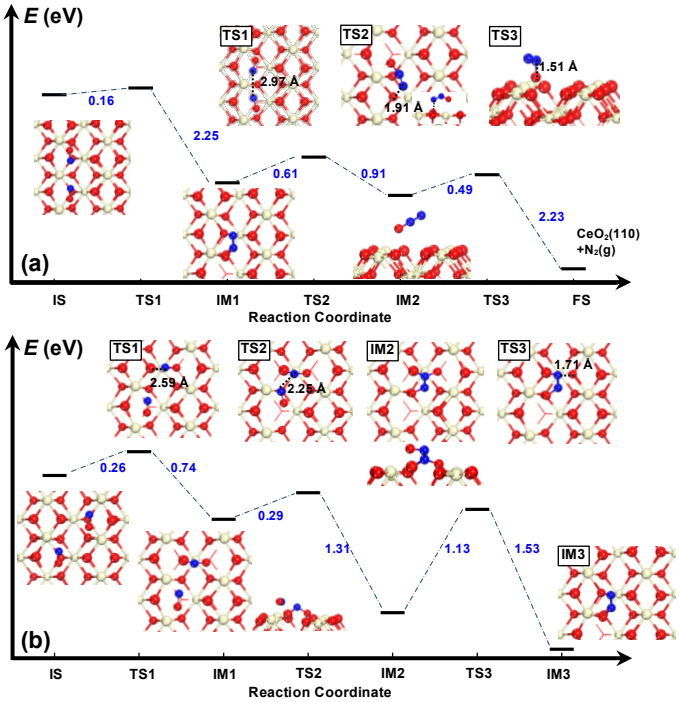

Fig. 3 Calculated energy profiles and key states of NO combination and N_2O_2 decomposition on O_A-O_D (a) and O_A-O_E (b) vacancy pairs. Two NO co-adsorption on vacancy pairs is set to energy zero.

From careful analyses, we found that the feasible occurrence of these processes and various corresponding surface intermediate species can be attributed to the unique electronic properties of the rare earth oxide support. In Table 2, we list the calculated electronic structures of various surface states and intermediate species of the reactions. As one can see, for the CeO_2(110) with a single O vacancy, there are two reduced Ce^{3+} occurring at the surface (see Table 2 and Fig. S3(a) for DOS and electron isosurface), which is very similar to the case of reduced CeO_2(111).[11] After NO adsorption, one of the two localized 4*f* electrons transfers to NO, and as the result, the negatively charged NO^- sits at the O vacancy by forming electrostatic attraction with the exposed Ce^{4+} cations (see Fig. S3(b)). Following the reaction between the adsorbed NO and nearby lattice O, the NO_2 still takes one electron, and accordingly, two more Ce^{3+} occur at the surface (Fig. S3(d)). We may therefore write this combination reaction as $NO^-+O^{2-}+2Ce^{4+}\rightarrow NO_2^-+2Ce^{3+}$. As we have discussed, such combination reactions are key to the migration of NO and their further reactions. Our calculations also showed that the corresponding barriers are quite low, *i.e.* 0.16 and 0.37 eV along [001] and [1$\bar{1}$0] directions, respectively. Interestingly, from further analyses, we found that at the transition states, the NO^- actually returns the electron to the surface, so that two Ce^{3+} occur again, and without the unfavourable electrostatic repulsion between NO^- and the reacting lattice O^{2-}, the NO+O^{2-} combination (see Fig. S3(c)) can therefore readily proceed with very low barriers. In other words, the capacity of surface Ce cation's 4*f* orbital to *reversibly* or *selectively* store and release electrons can have profound effect on both stabilizing the adsorbed reactants and promoting their reactions.

Table 2. Calculated number of surface Ce^{3+} ions and Bader charge of various NO_x adsorption state during NO decomposition process

	State	Number of Ce^{3+}	Bader charge	Figure
1Ov	Single O_v	2	/	S3(a)
	$NO_{(ad)}$	1	-0.72e	S3(b)
	TS of NO oxidation	2	-0.30e	S3(c)
	$NO_{2(ad)}$	3	-0.92e	S3(d)
2Ov	O_A-O_D vacancy pair	4	/	S3(e)
	$N2O2_{(ad)}$	2	-1.40e	S3(f)

Moreover, during further reactions between surface NO molecules, the N_2O_2 dimer is a key intermediate. As we have listed in Table 2, the original CeO_2(110) with two O vacancies contains 4 localized 4*f* electrons (or Ce^{3+} cations) (see Fig. S3(e)). By transferring 2 electrons to the N_2O_2 dimer, the surface not only increases the N-N bonding strength within the dimer,[21] and it also increases the electrostatic interaction between $N_2O_2^{2-}$ and surface cations at the vacancy (see Fig. S3(f)), which facilitates both the extraction of O from the dimer and formation of N_2.

In summary, through DFT+U calculations, we found that NO accommodated by O vacancy can readily diffuse at the reduced CeO_2(110) via alternative NO_2 formation and dissociation, and it can help N_2O_2 dimer formation and subsequent reduction to N_2. More importantly, the unique electronic properties of rare earth ceria play an important catalytic role in both *static* and *dynamic* ways by tuning the electron distribution in adsorbed reactants and reacting molecules, which can promote both the adsorption and activation of NO_x and their reactions.

This work was supported by the National Basic Research Program (2010CB732300, 2011CB808505), National Natural Science Foundation of China (21322307), Fundamental Research Funds for the Central Universities, Open Project of State Key Laboratory of Chemical Engineering (SKL-ChE-12C02) and Shanghai Rising-Star Program (12QH1400700). The authors also thank the National Super Computing Center in Jinan for computing time.

Notes and references

[a] *Key Laboratory for Advanced Materials and Research Institute of Industrial Catalysis, East China University of Science and Technology, 130 Meilong Road, Shanghai 200237, P.R. China*

[b] *State Key Laboratory of Chemical Engineering and Centre for Computational Chemistry, East China University of Science and Technology, 130 Meilong Road, Shanghai 200237, P.R. China*

[*] *Corresponding authors: xgong@ecust.edu.cn, gzhlu@ecust.edu.cn*

† Electronic Supplementary Information (ESI) available. See DOI: 10.1039/c000000x

1 M. Kang, D. J. Kim, E. D. Park, J. M. Kim, J. E. Yie, S. H. Kim, L. Hope-Weeks and E. A. Eyring, *Appl. Catal., B*, 2006, **68**, 21.
2 G. Liu and P. X. Gao, *Catal. Sci. Tech.*, 2011, **1**, 552.
3 N. Imanaka and T. Masui, *Appl. Catal., A*, 2012, **431–432**, 1.
4 M. Haneda, G. Tsuboi, Y. Nagao, Y. Kintaichi and H. Hamada, *Catal. Lett.*, 2004, **97**, 145.
5 J. Kaspar, P. Fornasiero and M. Graziani, *Catal. Today*, 1999, **50**, 285.
6 A. Trovarelli, C. de Leitenburg, M. Boaro and G. Dolcetti, *Catal. Today*, 1999, **50**, 353.
7 J. Kaspar, P. Fornasiero and N. Hickey, *Catal. Today*, 2003, **77**, 419.
8 N. Ta, J. Y. Liu and W. J. Shen, *Chin. J. Catal.*, 2013, **34**, 838.
9 H. F. Wang, Y. L. Guo, G. Z. Lu and P. Hu, *Angew. Chem. Int. Ed.*, 2009, **48**, 8289.
10 M. Nolan, S. C. Parker and G. W. Watson, *Surf. Sci.*, 2005, **595**, 223.
11 H. Y. Li, H. F. Wang, X. Q. Gong, Y. L. Guo, Y. Guo, G. Z. Lu and P. Hu, *Phys. Rev. B*, 2009, **79**, 193401.
12 F. Chen, D. Liu, J. Zhang, P. Hu, X. Q. Gong and G. Lu, *Phys. Chem. Chem. Phys.*, 2012, **14**, 16573.
13 Y. L. Song, L. L. Yin, J. Zhang, P. Hu, X. Q. Gong and G. Z. Lu, *Surf. Sci.*, 2013, **618**, 140.
14 M. Daturi, N. Bion, J. Saussey, J. C. Lavalley, C. Hedouin, T. Seguelong and G. Blanchard, *Phys. Chem. Chem. Phys.*, 2001, **3**, 252.
15 A. Martinez Arias, J.Soria, J. C. Conesa, X. L. Seoane, A. Arcoya and R. Cataluna, *J. Chem. Soc., Faraday Trans.*, 1995, **91**, 1679.
16 G. S. Qi, R. T. Yang and R. Chang, *Appl. Catal., B*, 2004, **51**, 93.
17 W. J. Hong, M. Ueda, S. Iwamoto, S. Hosokawa, K. Wada and M. Inoue, *Catal. Lett.*, 2012, **142**, 32.
18 A. Gayen, T. Baidya, G. S. Ramesh, R. Srihari and M. S. Hegde, *J. Chem. Soc.*, 2006, **118**, 47.
19 K. Zhou, X. Wang, X. Sun, Q. Peng and Y. Li, *J. Catal.*, 2005, **229**, 206.
20 W. J. Zhu, J. Zhang, X. Q. Gong and G. Lu, *Catal. Today*, 2011, **165**, 19.
21 Z. Yang, T. K. Woo and K. Hermansson, *Surf. Sci.*, 2006, **600**, 4953.
22 J. He, G. K. Reddy, S. W. Thiel, P. G. Smirniotis and N. G. Pinto, *Energy Fuels*, 2013, **27**, 4832.
23 M. Nolan, *Chem. Phys. Lett.*, 2010, **499**, 126.
24 J. Kullgren, K. Hermansson and C. Castleton, *J. Chem. Phys.*, 2012, **137**.
25 M. Haneda, Y. Kintaichi and H. Hamada, *Phys. Chem. Chem. Phys.*, 2002, **4**, 3146.
26 H. Y. Li, H. F. Wang, Y. L. Guo, G. Z. Lu and P. Hu, *Chem. Commun.*, 2011, **47**, 6105.
27 M. Nolan, J. E. Fearon and G. W. Watson, *Solid State Ionics*, 2006, **177**, 3069.
28 M. Haneda, Y. Kintaichi and H. Hamada, *Appl. Catal., B*, 2005, **55**, 169.
29 M. Haneda, T. Morita, Y. Nagao, Y. Kintaichi and H. Hamada, *Phys. Chem. Chem. Phys.*, 2001, **3**, 4696.
30 E. Ito, Y. J. Mergler, B. E. Nieuwenhuys, H. van Bekkum and C. M. van den Bleek, *Microporous Mater.*, 1995, **4**, 455.